Journal of Cellular Physiology

Visualization of Rab3A Dissociation During Exocytosis: A Study by Total Internal Reflection Microscopy

C.-C. LIN,[1,3,4]* C.-C. HUANG,[2] K.-H. LIN,[2] K.-H. CHENG,[2] D.-M. YANG,[5] Y.-S. TSAI,[6] R.-Y. ONG,[4] Y.-N. HUANG,[6] AND L.-S. KAO[1,2,3]*

[1]*Department of Life Sciences and Institute of Genome Sciences, National Yang-Ming University, Taipei, Taiwan, ROC*

[2]*Institute of Biochemistry, School of Life Sciences, National Yang-Ming University, Taipei, Taiwan, ROC*

[3]*Brain Research Center, University System of Taiwan, Hsinchu, Taiwan, ROC*

[4]*Department of Life Sciences, Chung Shan Medical University, Taichung, Taiwan, ROC*

[5]*Department of Medical Research and Education, Taipei Veterans General Hospital, Taipei, Taiwan, ROC*

[6]*Graduate Institute of Biomedical Engineering, Chung Yuan Christian University, Jhongli, Taoyuan, Taiwan, ROC*

Rab3A is a small G protein in the Rab3 subfamily, and is thought to act at late stage of exocytosis. However, the detailed mechanism of its action is not completely understood. To study the role of Rab3A in exocytosis, we used a total internal reflection fluorescence microscope to examine the fluorescence changes of EGFP-Rab3A-labeled and NPY-EGFP-labeled vesicles in PC12 cells upon stimulation. The fluorescence of EGFP-Rab3A-labeled and NPY-EGFP-labeled vesicles decreased while showing different patterns. The NPY-EGFP-labeled vesicles that exocytosed showed a transient fluorescence increase before NPY-EGFP fluorescence disappearance, which represents fusion and NPY release. This transient increase was diminished in cells that co-expressed the GDP-bound Rab3A mutant. The fluorescence of EGFP-Rab3A-labeled vesicles dispersed before disappearance, which represents the dissociation of Rab3A from the vesicles. The dispersion was not found in GTP-bound Rab3A mutant-labeled vesicles. Interestingly, EGFP-Rab3A F59S, a mutant unable to bind rabphilin, dissociates slower from the vesicles than wild type Rab3A and caused a slower release of NPY-EGFP. The results provide direct evidence to support the hypothesis that GTP hydrolysis and rabphilin are involved in Rab3A dissociation from the vesicles and the occurrence of exocytosis.

J. Cell. Physiol. 211: 316–326, 2007.

Exocytotic secretion of neurotransmitters and hormones is a fundamental step in synaptic neurotransmission and cell–cell communication and involves sequential steps of complex protein–protein interactions. The late steps of exocytosis include the translocation, docking and priming of the secretory vesicles before fusion and release of neurotransmitters (for a review see Südhof, 2004). Molecules involved in these steps have been identified by biochemical and molecular biological approaches. However, the functions of each molecule and the interactions among molecules have been difficult to study due to the lack of proper techniques that are able to examine the events occurring near the plasma membrane in a real-time manner. Recent advances in optical methods and fluorescent proteins now allow a direct observation of molecules in a living cell with adequate temporal and spatial resolution. Specifically, total internal reflection fluorescence microscope (TIRFM) has been used successfully to examine the exocytosis of single vesicles in several cell types (e.g., Steyer et al., 1997; Taraska et al., 2003; Ohara-Imaizumi et al., 2004). In this study, we used TIRFM to study the role of Rab3A in the late steps of exocytosis. Rab3A, one member in the small G protein Rab family, is predominantly expressed in neurons and secretory cells, and is thought to be involved in the late steps of exocytosis. Rab3A binds to the secretory vesicles via C-terminal geranylgeranyl moieties (Johnston et al., 1991), and cycles between an active secretory vesicle-associated GTP-bound form and an inactive cytosolic GDP-bound form (see Macara, 1994). It is generally thought that during secretion GTP hydrolysis occurs and the resulting GDP-Rab3A dissociates from the vesicles by forming a complex with guanine nucleotide dissociation inhibitor (GDI). The GDP-Rab3A is then reattached to the vesicles and is converted into GTP-Rab3A by the guanine nucleotide exchange protein through mechanisms largely unknown (for a review see

C.-C. Lin and C.-C. Huang contributed equally to this work.

This article includes supplementary material, available from the authors upon request or via the Internet at http://www.interscience.wiley.com/jpages/0021-9541/suppmat.

Contract grant sponsor: National Science Council, ROC;
Contract grant numbers: NSC89-2311-B-040-005, NSC-90-2311-B-040-006, NSC 92-2311-B-040-006, NSC 93-2311-B-010-016, NSC95-2320-B-010-020.
Contract grant sponsor: Brain Research Center, University System of Taiwan, Taiwan, ROC.
Contract grant sponsor: Ministry of Education, ROC.
Contract grant sponsor: Aim for the Top University Plan.
Contract grant sponsor: Chung Shan Medical University, Taichung, Taiwan, ROC;
Contract grant number: CSMU91-OM-B-014.

R.-Y. Ong's present address is Institute of Neuroscience, National Yang-Ming University, Taipei, Taiwan, ROC.

*Correspondence to: L.-S. Kao and C.-C. Lin, Department of Life Sciences, School of Life Sciences, National Yang-Ming University,Taipei 112, Taiwan, ROC. E-mail: lskao@ym.edu.tw; cclin2@ym.edu.tw

Received 22 February 2006; Accepted 11 October 2006

DOI: 10.1002/jcp.20938

Geppert and Südhof, 1998). However, most of the above results were obtained by in vitro biochemical analysis; there is no direct evidence to correlate the Rab3A cycle and the individual steps in the secretory process.
Previous evidence supports multiple roles for Rab3A in the secretory process. First, it appears that Rab3A is involved in the recruitment or docking of the vesicles from the reserved pool. In Rab3A-knockout mice, the cytosolic distribution of synaptic vesicles is similar to that of the wild-type, but after secretion fewer vesicles are present in the active zone (Leenders et al., 2001) and synaptic depression is increased after repetitive stimulation (Geppert et al., 1994). Second, Rab3A is thought to serve as a gatekeeper at a late stage of exocytosis. Overexpression or microinjection of Rab3A or a GTPase-deficient mutant of this protein inhibits regulated exocytosis in chromaffin cells and PC12 cells (Holz et al., 1994; Johannes et al., 1994; Lin et al., 1996, Schlüter et al., 2002). In hippocampal neurons of Rab3A knockout mice, Ca^{2+}-dependent exocytosis is increased (Geppert et al., 1997). Third, Rab3 modulates the activity of the fusion machinery by controlling the formation or the stability of the SNARE complex, although it is not clear whether the effect is exerted directly by Rab3A or through effectors (Johannes et al., 1996; Coppola et al., 2002). Finally, Rab3A may also be involved in endocytosis or the recycling of vesicles, possibly mediated by its putative effector, rabphilin, through interaction with rabaptin-5 (Ohya et al., 1998; Coppola et al., 2001). Moreover, Rab3A has been shown to localize to endosomes in resting chromaffin cells (Slembrouck et al., 1999). In this study, we used TIRFM to visualize the localization and fluorescence changes of fluorescent protein-tagged Rab3A and its mutants during secretion in PC12 cells. Furthermore, to study how Rab3A cycle affects secretion, we co-expressed Rab3A or its mutants with NPY-EGFP, a marker for the secretory vesicles and the secretory process, in PC12 cells. Our results provide direct evidence to support the hypothesis that the hydrolysis of GTP and interaction with rabphilin are important for the dissociation of Rab3A from the vesicles and the occurrence of exocytosis.

Materials and Methods

Plasmids and cell culture

PC12 cells, a rat adrenal pheochromocytoma cell line, were obtained from the American Type Culture Collection (ATCC, Rockville, MD). PC12 cells were cultured in Dulbecco's Modified Eagle Medium (DMEM) containing 10% horse serum (heat-inactivated) and 5% fetal bovine serum as described previously (Yang et al., 2003). Cells were plated on poly-L-lysine coated 24 mm coverslips in 35 mm culture dishes at a density of 3×10^5 cells per dish.
Rat Rab3A was subcloned into either pECFP (cyan fluorescence protein)-C1 or pEGFP (green fluorescence protein)-C1 (Clontech, Palo Alto, CA) with the N-terminus fused in frame to the C-terminus of ECFP or EGFP (Yang et al., 2003). EYFP-ER was obtained from Clontech.

Transfection

PC12 cells were transfected with plasmids using LipofectAmine-2000® reagent (Gibco, Carlsbad, CA) as described previously (Yang et al., 2003). Briefly, 1 μg of the desired DNA was diluted into 1 ml serum-free DMEM and then mixed well with 3 μl of the LipofectAmine-2000®. The solution was incubated for at least 20 min before adding the mixture to the cells. Cells were incubated at 37°C in a CO_2 incubator for 1 h, then 1 ml DMEM containing 20% horse serum and 10% fetal bovine serum was added. After 5 h, the medium was changed with fresh serum-containing medium. The transfected cells were used for the experiments after 2 days.

Immunocytochemistry and fluorescence microscopy

PC12 cells were fixed with paraformadehyde (3.7% in PBS, phosphate-buffered saline containing 136.89 mM NaCl, 2.68 mM KCl, 8.09 mM Na_2HPO_4 and 1.76 mM KH_2PO_4). They were then, stained with a mouse monoclonal anti-Rab3A antibody (1:200, BD Bioscience, Palo Alto, CA) and then rhodamine-conjugated anti-mouse secondary antibody (1:200, Jackson Lab, Inc., West Grove, PA).
Transfected PC12 cells on coverslips were incubated in control buffer (150 mM NaCl, 5 mM KCl, 1 mM $MgCl_2$, 2.2 mM $CaCl_2$, 5 mM glucose, and 10 mM HEPES, pH 7.4) and examined at room temperature by an inverted epifluorescence microscope (IX-70, Olympus Optical Co., Ltd, Tokyo, Japan) equipped with a 100X objective (UPlanApo, NA1.35, Olympus Optical Co., Ltd). Time-dependent images were acquired by a cooled CCD camera (MicroMAX 782 YHS, Princeton Instruments, Roper Scientific, Inc., Trenton, NJ).
The confocal laser scanning microscope (FluoVIEW FV-300, Olympus Optical Co., Ltd) used an argon 488 nm laser (10 mW, Melles Griot, Irvine, CA) to excite EGFP and a He-Ne 543 nm laser (1 mW, Melles Griot) to excite rhodamine.

Stimulation of PC12 cells

Cells were stimulated by a 2 sec pulse of high K^+ buffer (150 mM KCl in a buffer containing 5 mM NaCl, 1 mM $MgCl_2$, 2.2 mM $CaCl_2$, 5 mM glucose, 10 mM HEPES, pH 7.4) or a 6 sec pulse of 200 μM ATP applied through an ejection micropipette at a positive pressure of 10 psi (Picospritzer II, Paker Hannifin, Cleveland, OH). The micropipette was pulled from a glass capillary by a micropipette puller (P-97, Sutter, Novato, CA). The tip of the micropipette (o.d. 2 μm) was polished using a microforge (MF-83, Narishige, Tokyo, Japan). The ejection micropipette was held by a micromanipulator (MHW-3, Narishige) and positioned at a distance of approximately 10 μm from the cell.

Setup for TIRFM

The objective-type TIRFM system was setup on an inverted microscope (IX-71, Olympus Optical Co., Ltd). The dual port TIRF/Epi condenser (T.I.L.L. Photonics, Gräfelfing, Germany) was coupled with an Argon-Krypton 488 nm laser (NEC, Tokyo, Japan) and a Xenon lamp (Polychrome IV, T.I.L.L. Photonics) as light sources. Through a high numerical aperture objective (PlanApo 60x, NA 1.45 Oil, Olympus Optical Co., Ltd), the laser beam was bent by the TIRF condenser to produce a thin illumination range ($<$90 nm) in the z-axis relative to the coverslip. Both TIRFM and epi-fluorescence images were acquired using a fast cooled CCD (IMAGO QE, T.I.L.L. Photonics) controlled by commercial software (TILLvisION 4.0, T.I.L.L. Photonics), which also controlled the related hardware including the shutters for the laser and the Xenon lamp. The TIRFM images were acquired at $\sim$2 frames/sec. For background correction, the average background intensity measured in a region outside the cells, and that in a region without vesicles in the cell were subtracted before measurements of total fluorescence in the evanescent field and the fluorescence of single vesicles, respectively.

Analysis of the TIRFM images

Total fluorescence in the evanescent field and fluorescence of single vesicle were analyzed using commercial software: MetaMorph 5.0 (Universal Imaging, Downingtown, PA) and DiaTrack 3.0 (Semasopht, Chavannes, Switzerland). DiaTrack is able to track single vesicles automatically using the pixel that showed highest fluorescence intensity. The fluorescence spots on first frame of the TIRFM images were first identified by DiaTrack. The spots identified were then confirmed and those that appeared to be artifacts were removed manually before automatic tracking proceeded. The vesicles that showed fluorescence changes were identified by comparing the first frame and last frame analyzed, and the vesicles that had disappeared were selected. Fluorescence change of a single vesicle was also analyzed by MetaMorph (Fig. 6B). Vesicles that proceed to exocytosis were initially selected subjectively from the TIRFM images. The coordinates and time of occurrence of each event were marked and a square of 1.2×1.2 μm was placed around the event and the fluorescence was quantified. Only vesicles present from the first frame that show changes were chosen and vesicles that were not present in the squares of all frames were deleted. Although the results obtained using the two types of software were similar, it should be noted that individual vesicle were represented by the pixel with highest fluorescence intensity when analyzed by DiaTrack, while MetaMorph measured the total fluorescence of the vesicle in the region of interest defined and this is shown as the average fluorescence/pixel.

Results

Fluorescent protein-tagged Rab3A and NPY showed punctuate patterns when overexpressed in PC12 cells

The subcellular localization of fluorescent protein-fused Rab3A and NPY when overexpressed in PC12 cells was first examined. NPY-EGFP was used as a fluorescent marker for the dense core secretory granules in PC12 cells (Lang et al., 1997). The vesicles that were labeled by Rab3A and NPY were detected by a confocal microscope. NPY-EGFP was observed directly by EGFP fluorescence and Rab3A was revealed by immunostaining with a polyclonal anti-Rab3A antibody (Fig. 1).
Both NPY-EGFP fluorescence and Rab3A immunostaining showed punctuate patterns and the staining was more concentrated near plasma membrane and processes than in the cytosol (Yang et al., 2003). The two molecules were partially co-localized (Fig. 1A,B). These results were expected because overexpressed Rab3A in PC12 cells has been shown to be associated with both synaptic-like microvesicles and large dense core vesicles (Matteoli et al., 1991; Chung et al., 1999), whereas NPY-EGFP is present mainly in the dense core vesicles (Lang et al., 1997). However, whether Rab3A associates with the entire population or only a subpopulation of secretory vesicles, such as vesicles in the releasable pool, is not clear.

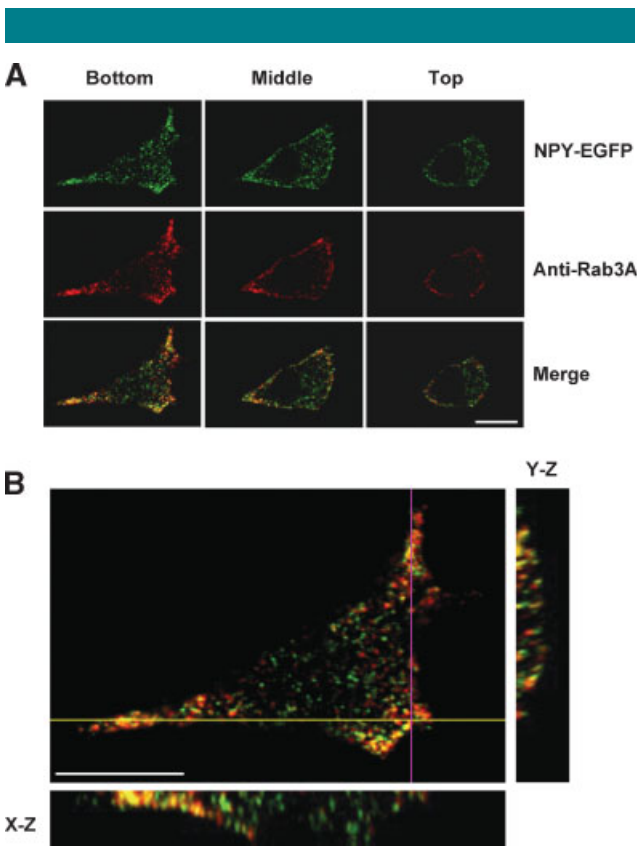

Fig. 1. Subcellular localization of ECFP-Rab3A and NPY-EGFP in PC12 Cells. NPY-EGFP and ECFP-Rab3A were co-expressed in PC12 cells. Due to the limitation of the laser available on our confocal microscope, NPY-EGFP was viewed directly by its fluorescence using the argon laser and ECFP-Rab3A was detected by immunostaining with anti-Rab3A antibodies and rhodamine-conjugated secondary antibodies and then examined by confocal fluorescence microscope. Pseudocolored images are shown: green for fluorescence of NPY-EGFP and red for Rab3A. A: The top, middle and bottom confocal sections of PC12 cells were shown as indicated. B: Confocal sections were either rendered into 2D images in x-y direction or reconstructed into a 3D image to view two regions of the cells (marked by lines) in x-z and y-z directions. Bar: 5 μm.

When ECFP-Rab3A and EGFP-Rab3A were used in this study; the fluorescence images from them completely overlapped with those obtained by staining with the anti-Rab3A antibodies (data not shown).

Changes of NPY-EGFP fluorescence upon stimulation—analysis of total fluorescence in the evanescent field

The fluorescence change of NPY-EGFP-labeled vesicles upon stimulation monitored by TIRFM was characterized first. Total fluorescence of the cell in the evanescence field was analyzed, which represents the overall change of the NPY-EGFP-labeled vesicles near the plasma membrane (Fig. 2A and Video 1). High K^+ stimulation induced a decrease in the total fluorescence and about 40% of the cells examined showed a transient increase before the decrease (Fig. 2A). The control buffer did not have any significant effect on the fluorescence of NPY-EGFP (Fig. S1A). To confirm that the decrease is specific for NPY-EGFP labeled vesicles, a control was carried out by expressing an ER-targeted fluorescent protein, EYFP-ER and no significant change in the fluorescence was detected under the same experimental conditions (data not shown).
The NPY-EGFP fluorescence decreased upon stimulation due to the release of NPY-EGFP as expected. The transient increase in the NPY-EGFP fluorescence appeared to be due to an increase in intravesicular pH during exocytosis and the change occurs because EGFP is known to be sensitive to pH (Patterson et al., 1997). Stimulation induced the opening and expansion of the fusion pore to allow a pH increase in the vesicle, which caused the transient increase in the NPY-EGFP fluorescence (Barg et al., 2002; Taraska et al., 2003; Perrais et al., 2004). The subsequent release of NPY-EGFP caused the decrease of fluorescence. For the cells that showed fluorescence decrease without the transient increase, we were still able to detect the brightening of individual vesicles (see below).

Changes of NPY-EGFP fluorescence upon stimulation—analysis of single vesicle fluorescence

To further understand how the individual vesicles behave, the fluorescence changes of individual vesicles present in the evanescent field were analyzed (Fig. 2B–D and Video 2). The fluorescence of most vesicles tracked did not change significantly. When 1271 NPY-EGFP-labeled vesicles tracked from 9 cells, we were able to identify 71 vesicles that disappeared upon stimulation, while only 1 vesicle disappeared during the resting state over the same time period (20 sec after stimulation). The fluorescence changes can be divided into three patterns. In type 1, where 16 vesicles showed a fluorescence increase to more than twofold of the initial level and then gradually decreased with the residual fluorescence intensity being higher than the initial level (top parts, Fig. 2C,D), which has been suggested to result from the vesicles resealing after kiss-and-run type exocytosis. NPY-EGFP fluorescence increased due to the pH increase in the vesicle during the brief opening of the fusion pore and then decrease after resealing and reacidification of the interior of the vesicle (Barg et al., 2002; Taraska et al., 2003; Perrais et al., 2004). In type 2 (25 vesicles), there was a transient fluorescence increase and then the fluorescence of NPY-EGFP vesicles decreased rapidly to the background value in about 3 sec (middle parts, Fig. 2C,D). This transient fluorescence increase is different from the type 1 change; the transient increase occurred in <1 sec and the extent of the increase was smaller, being about $55.4 \pm 7.8\%$ of the initial value (see below). In the case of type 3 events (30 vesicles), the fluorescence decreased abruptly to the background level within 0.5 sec (bottom parts, Fig. 2C,D). The decrease is possibly caused by the release of NPY-EGFP that was too fast to be caught at the temporal resolution used.

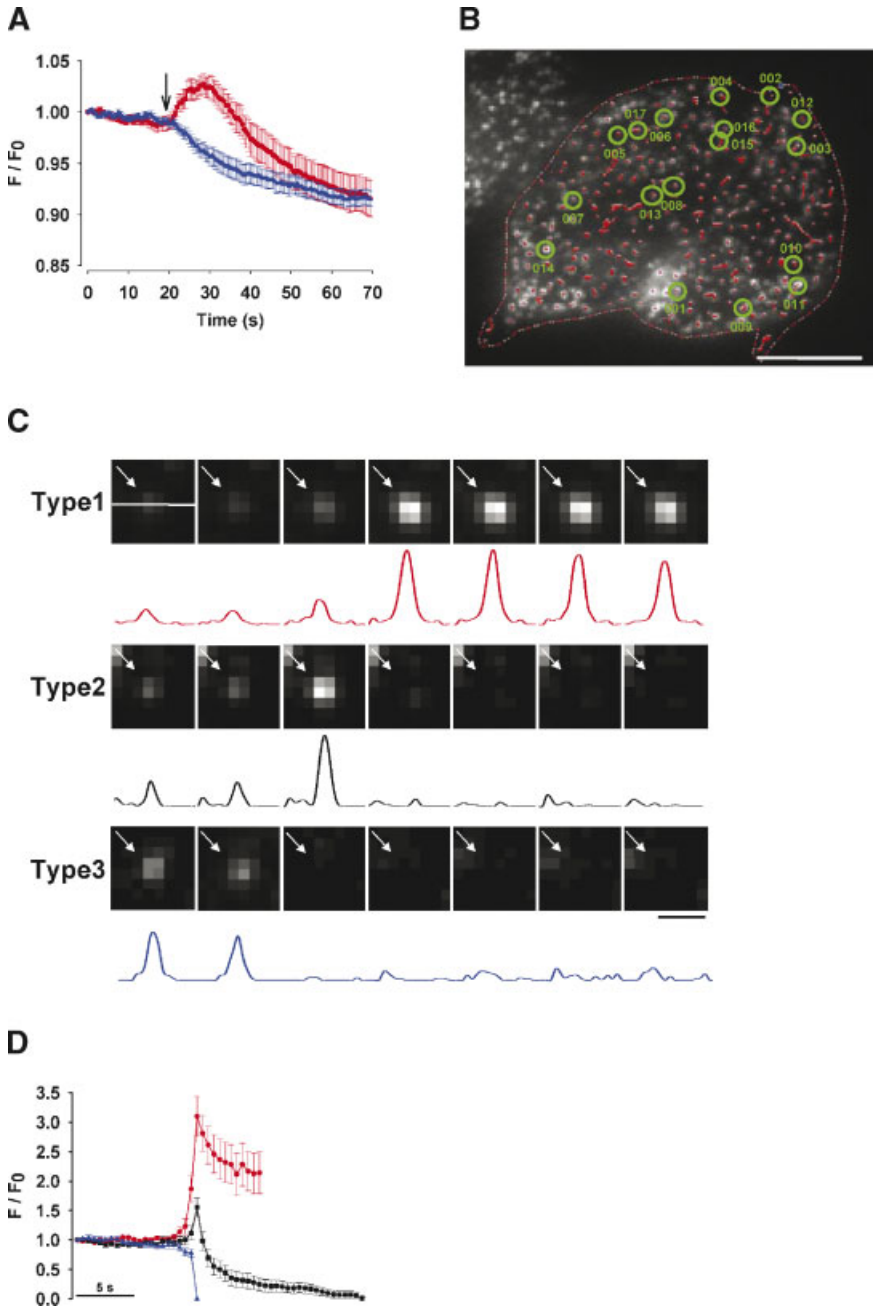

Fig. 2. Changes in the fluorescence of NPY-EGFP-labeled vesicles during secretion. PC12 cells were transfected with pNPY-EGFP. The transfected cells were stimulated by high K^+ for 2 sec and fluorescence images were acquired by TIRFM. A: Total fluorescence in the evanescent field. The decrease in the fluorescence upon stimulation, at the arrow, was classified into the ones with (●) and without (○) transient effects. Total fluorescence in the evanescent field was measured from 29 cells that showed fluorescence change upon stimulation by MetaMorph. Fluorescence (F) was normalized to the first frame at resting level (F_0). The data shown are the mean ± SEM from 11 cells with transient effects and 18 cells without transient effects from six independent transfection experiments. B: A representative cell that showed the trajectories of the vesicles identified and these were tracked in 30 sec. Vesicles were tracked and the fluorescence of single vesicles was analyzed by DiaTrack as that described in Materials and Methods. Vesicles circled are those analyzed. C: Changes in the single vesicle fluorescence. Representative images of single vesicles showing the different patterns of fluorescence changes. In total, 71 vesicles out of 1,271 vesicles from 9 cells were tracked and showed significant fluorescence changes; these were classified into three major patterns: type 1, fluorescence increase before decrease to the level above the initial fluorescence (top parts); type 2, transient increase before decrease to the background level (middle parts); and type 3, abrupt decrease (bottom parts). Traces under each image show the fluorescence intensity of the individual pixels scanned across the center of the vesicle (indicated by the white line). Black bar: 0.5 μm. D: Averaged fluorescence changes of single vesicles. Vesicles with different patterns of fluorescence changes were grouped and averaged. The fluorescence of individual vesicles was aligned first before averaging: type 1 (●) change was aligned at the frame with highest fluorescence intensity and type 2 (□) and 3 (▲) were aligned at the frame before the fluorescence decrease. Fluorescence (F) was normalized to the first frame at resting level (F_0). Data shown mean ± SEM from 16 vesicles for type 1, 25 vesicles for type 2, and 30 vesicles for type 3.

Although the increase in intravesicular pH during exocytosis has been suggested to cause the type 2 transient fluorescence increase (Taraska et al., 2003; Allersma et al., 2004), it is also possible that vesicles move closer to the plasma membrane, which will allow more evanescent light to excite the NPY-EGFP. To examine these possibilities, NH_4Cl was added, which neutralized the acidic pH in the vesicles, and the NPY-EGFP fluorescence of individual vesicles was increased by about $29.1 \pm 4.2\%$, which is in a range similar to that reported previously (Sankaranarayanan et al., 2000). The subsequent stimulation induced an average increase of $58.0 \pm 9.4\%$ in the same population of vesicles (11 vesicles from 4 cells), a change that cannot be entirely accounted for by the change in pH. Furthermore, when the experiments were carried out in pH 5.5 buffer, a similar type 2 NPY-EGFP fluorescence transients as that which occurred in the control pH 7.4 buffer were still observed ($39.9 \pm 6.2\%$ vs. $44.3 \pm 7.9\%$ from 10 out of 22 vesicles analyzed in 3 cells that showed type 2 transient change). The transient change was expected to become smaller at pH 5.5 if it is caused by a pH change. Therefore, it is possible that the fluorescence transient was induced at least partly by the movement of the vesicles closer to the plasma membrane.

Changes of EGFP-Rab3A fluorescence upon stimulation—analysis of total fluorescence in the evanescent field

To study how the Rab3A-associated vesicles behave upon stimulation, changes in the fluorescence of PC12 cells that overexpressed EGFP-Rab3A upon stimulation were then monitored by TIRFM and compared with those of NPY-EGFP. Total fluorescence of the cell in the evanescence field was first analyzed and this represents the overall change of EGFP-Rab3A near the plasma membrane (Fig. 3A, Video 3). High K^+ stimulation induced a decrease in the EGFP-Rab3A fluorescence, which is Ca^{2+}-dependent because no fluorescence change was detected in Ca^{2+}-free buffer (data not shown). About half of the cells analyzed showed a transient increase before the decrease. The control buffer did not have any significant effect on the fluorescence (Fig. S1B). Stimulation induced a decrease in the NPY-EGFP fluorescence as shown in Figure 2A; this is expected as NPY-EGFP is released during exocytosis (Taraska et al., 2003). However, it is surprising that the EGFP-Rab3A fluorescence in the evanescent field also decreased. To determine whether this decrease in fluorescence was due to EGFP-Rab3A being secreted out of the cells or because it simply leaves the evanescent field but remained in the cell after stimulation, the fluorescence of EGFP-Rab3A in PC12 cell was monitored by an epifluorescence microscope using a low magnification, low NA value lens (20X/dry/NA 0.75, the depth of field at 500 nm is 1.35 μm) and no significant change of fluorescence occurred upon stimulation (data not shown). Therefore, upon stimulation Rab3A left the evanescent field but remained in the cell.

Changes of EGFP-Rab3A fluorescence upon stimulation—analysis of single vesicle fluorescence

To understand how Rab3A may behave during secretion, the stimulation-triggered fluorescence changes of EGFP-Rab3A-labeled vesicles were then analyzed at the single vesicle level. The fluorescence of single vesicles that showed disappearance upon stimulation, presumably representing those that underwent exocytosis, were analyzed. For EGFP-Rab3A-labeled vesicles, out of a total 2,897 vesicles tracked in 14 cells (ranging from 89 to 363 vesicles/cell), we were able to identify 129 vesicles that showed a decrease of fluorescence in the 20 sec after stimulation (Fig. 3B). Interestingly, the patterns of fluorescence change were very different from those of NPY-EGFP-labeled vesicles (Fig. 3C,D, Video 4). The fluorescence of EGFP-Rab3A gradually dispersed into a larger area first before completely disappearing, which is likely to correlate with the dissociation of Rab3A (top parts, Fig. 3C and lower curve, Fig. 3D). There were 18 EGFP-Rab3A-labeled vesicles that showed a slight increase in their fluorescence of about 15% of the initial vesicle fluorescence before disappearance (middle parts, Fig. 3C and upper curve, Fig. 3D). For the same cells stimulated with control buffer, only 5 vesicles show fluorescence change over the same time period monitored. When these vesicles were examined individually, the fluorescence spots became smaller and then disappeared suggesting that these vesicles left the evanescent field (bottom parts, Fig. 3C). Therefore, under TIRFM, it is possible to distinguish the two situations that account for the decrease of Rab3A fluorescence: with stimulation, it appeared that the dispersion of the fluorescence was caused by that Rab3A dissociating from the vesicle and diffusing away; without stimulation the vesicles along with the associated Rab3A simply left the evanescent field causing the fluorescence spot to become smaller rather than dispersing.

Effects of GTP hydrolysis and rabphilin on Rab3A dissociation

It is known that Rab3A cycles between GTP- and GDP-bound forms and requires several proteins for its function. To further understand how the cycle of GTP hydrolysis and rabphilin, a Rab3A effector, are involved in the fluorescence changes observed, Rab3A Q81L (a GTP-bound mutant), Rab3A T36N (a GDP-bound mutant), and Rab3A F59S (a mutant protein defective in GTP-dependent rabphilin binding), were overexpressed in PC12 cells and their fluorescence changes upon stimulation were examined. PC12 cells overexpressing Rab3A Q81L and Rab3A F59S showed similar punctuate patterns as the wild type Rab3A (Fig. 4A,B,D). The Rab3A T36N showed a diffuse pattern under TIRFM, the black patches representing plasma membrane that did not attach the substrate (Fig. 4C). Together with the results obtained by epifluorescence microscope (Fig. 4G), Rab3A T36N appeared to be localized in the plasma membrane and the cytosol. The fluorescence changes of EGFP-Rab3A and mutants in living PC12 cells upon stimulation were then monitored by TIRFM and recorded. Because Rab3A mutants inhibited secretion, to gain a larger and more reliable secretory response, cells were stimulated by puffing a 200 μM ATP solution onto the cells for 6 sec. The total fluorescence in the evanescent field of transfected cells was first analyzed (Fig. 5). In general, the total fluorescence in the evanescent field of Rab3A and the mutants also showed two major types of changes upon stimulation and these were decreases with and without transient increases, which is similar to that of wild-type (Fig. 3A and Fig. 5A,B). For the population of cells that showed a total fluorescence decrease without the transient increase (Fig. 5A), in the wild-type Rab3A-expressed cells the fluorescence decreased by about 13%. Approximately 25% of transfected cells showed a transient increase in fluorescence upon stimulation (Fig. 5B). The transient increase in the fluorescence appears to be due to some of the Rab3A-labeled vesicles in the evanescent field moved closer to the plasma membrane; this may represent the transport of vesicles toward their docking sites on the plasma membrane. The extent of the transient increase, about 3% of the initial fluorescence level, was similar for all the cells expressing Rab3A and the mutants.

In cells that expressed Rab3A Q81L, the extent of fluorescence decrease was less than that of the wild-type (Fig. 5A). The results are in accord with the lower level of exocytotic activity in these cells (Holz et al., 1994; Johannes et al., 1994; Schlüter et al., 2002). For cells with a transient fluorescence increase (Fig. 5B), the transients are slower and smaller compared to the

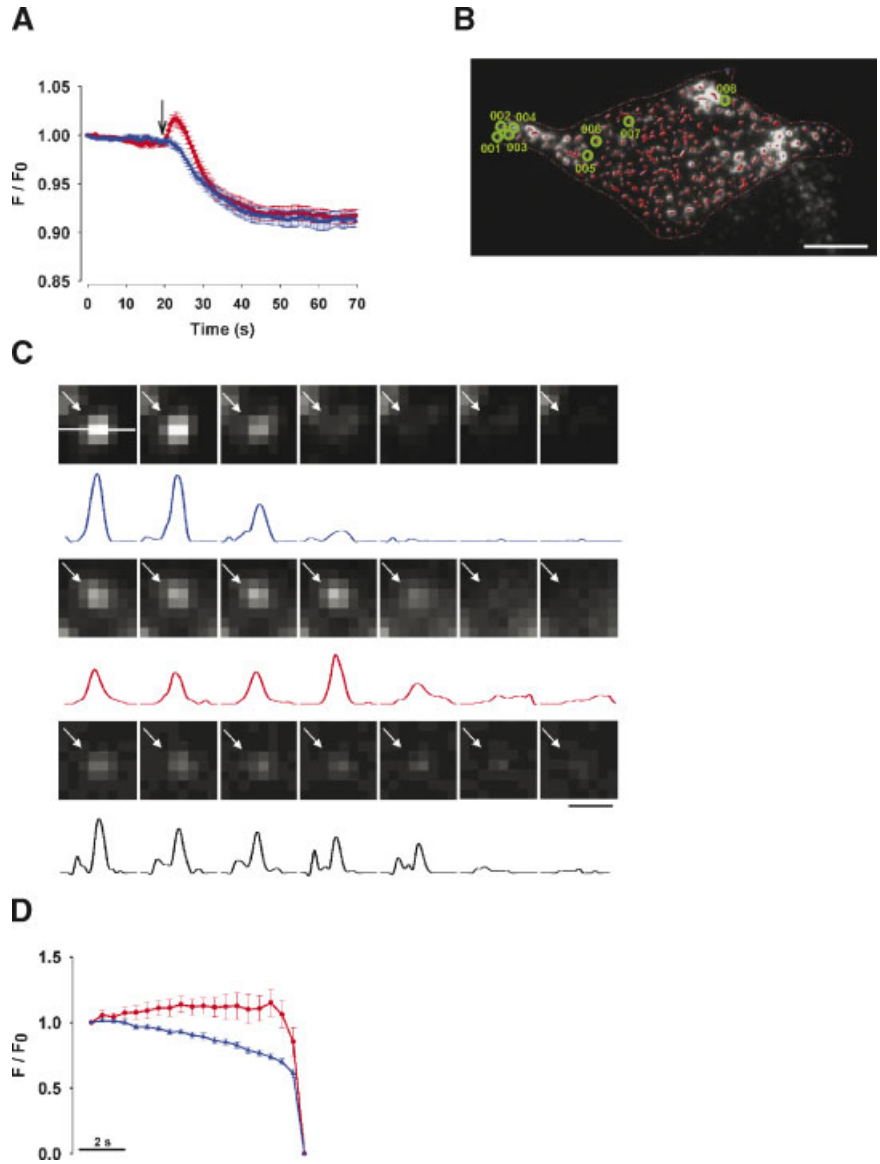

Fig. 3. Patterns of dissociation of Rab3A from vesicles during secretion. PC12 cells were transfected with pEGFP-Rab3A. The transfected cells were stimulated by high K^+ for 2 sec and fluorescence images were acquired by TIRFM. A: Total fluorescence in the evanescent field. The decrease in the fluorescence upon stimulation indicated by the arrow was classified into the ones with (●) and without (○) the transient increase. Total fluorescence in the evanescent field was measured by MetaMorph. Data shown are mean ± SEM from 22 cells with the transient effect and 23 cells without the transient effect from 8 independent transfection experiments. B: A representative cell showing the trajectories of vesicles was identified and tracked for 30 sec. Vesicles circled are those analyzed. Vesicles were tracked and the fluorescence of single vesicles was analyzed by DiaTrack as that described in Materials and Methods. C: Changes in the single vesicle fluorescence. Representative images of single vesicles that showed different patterns of fluorescence changes are shown. Fluorescence changes of single vesicles was analyzed: 2,897 vesicles from 14 cells were tracked and 129 vesicles disappeared and this was classified into two patterns: 111 vesicles showed a slow dispersion before an abrupt decrease to background (top parts) and 18 vesicles showed a small increase before dispersion and disappearance (middle parts). Bottom parts show the pattern of vesicle leaving the evanescent field. Traces under each image show the fluorescence intensity of the individual pixels scanned across the center of the vesicle (indicated by the white line). Bar: 0.5 μm. D: Averaged fluorescence changes of single vesicles. Vesicles with different patterns of fluorescence changes as described above were grouped and synchronized at the frame before the abrupt disappearance of fluorescence (△, the type with a slow dispersion before an abrupt decrease; ●, the type with a small increase before dispersion and disappearance). Fluorescence (F) was normalized to the level at resting level (F_0). The data shown are the mean ± SEM from number of vesicles described above.

wild-type, which seemed to be due to vesicles moving closer to and then away from the plasma membrane in the evanescent field. The results from single vesicles analysis correlates with the overall fluorescence change. The vesicles that disappeared were selected and their fluorescence intensity was measured. None of the 32 vesicles that were tracked showed fluorescence dispersion; the fluorescence disappeared within one frame, 0.5 sec. The vesicles that showed fluorescence decrease seemed to have moved away from the evanescent field because their area of the fluorescence became smaller (Fig. 5C). These results indicate that GTP hydrolysis is critical for the dissociation of Rab3A from the vesicles. Interestingly, for cells overexpressing Rab3A T36N, which is located on the plasma membrane (Fig. 4C,G), the total fluorescence in the evanescent field decreased upon stimulation (Fig. 5A), suggesting that the Rab3A T36N dissociation is Ca^{2+}-dependent.

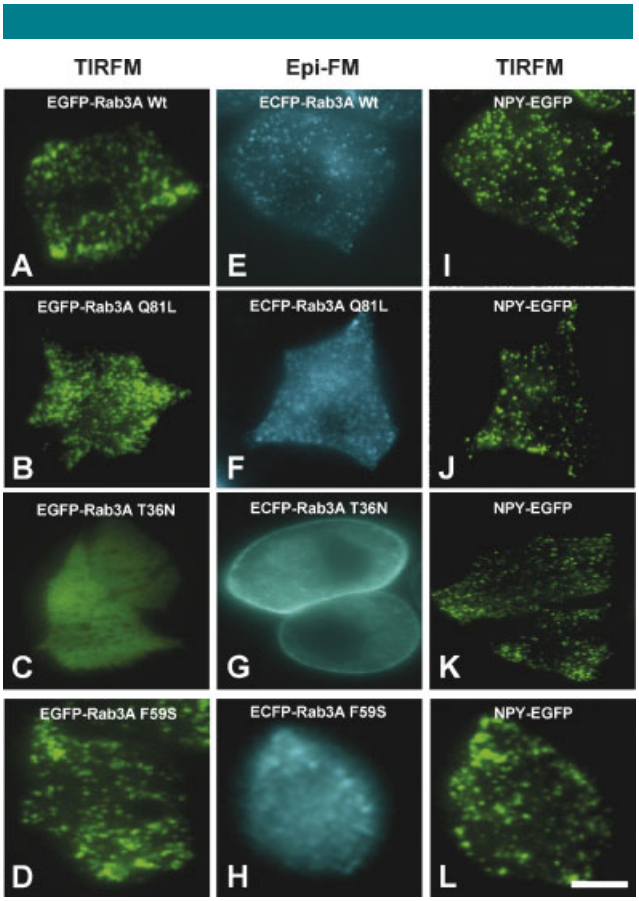

Fig. 4. Fluorescence patterns of PC12 cells that expressed NPY-EGFP and EGFP-Rab3A or its mutants. PC12 cells were transfected with pEGFP-Rab3A or its mutants (A–D) or co-transfected with pNPY-EGFP (E–H) and pECFP-Rab3A or its mutants (I–L). The fluorescence images were acquired by TIRFM and epi-fluorescence microscope as indicated. Bar: 5 μm.

For cells overexpressing Rab3A F59S, which are defective in the interaction of Rab3A with rabphilin, the extent of total fluorescence decrease in the evanescent field was less, and the transient effect appeared later compared to the wild type (Fig. 5A,B). When the fluorescence of single vesicles was examined, the Rab3A F59S fluorescence showed dispersion before disappearance (Fig. 5C). Furthermore, the dissociation of Rab3A F59S appears to occur in two phases; the molecule dissociated from the vesicles slowly initially and then an abrupt final dissociation occurred (Fig. 5D). These results suggest that the interaction with rabphilin affects the association of Rab3A and the vesicles, and the movement of vesicles to the docking site.

Effects of Rab3A and mutants on the release pattern of single NPY-EGFP vesicles

The role of Rab3A in the secretory pathway was further studied by co-expression of ECFP-Rab3A or its mutants with NPY-EGFP in PC12 cells. ECFP fluorescence was used to select the cells that expressed Rab3A or its mutants and then NPY-EGFP fluorescence was examined by TIRFM. The cells overexpressing the various Rab3A mutants did not show any significant effect on the punctuate pattern of NPY-EGFP fluorescence (Fig. 4I–L). Change in the total NPY-EGFP fluorescence in the evanescent field during secretion was then analyzed (Fig. 6A, Video 6–8). In most control PC12 cells that co-expressed with empty vector, ATP induced a transient increase in the NPY-EGFP fluorescence. The extent of fluorescence decrease appeared to be less in cells that co-expressed Rab3A Q81L and Rab3A F59S. When single vesicles were analyzed, except for cells overexpressing Rab3A T36N, where we did not find vesicles showing the type 1 change, the other cells showed the three types of fluorescence changes as described above (Fig. 2). When these vesicles were examined more carefully, it was possible to identify some subtle differences in the vesicles that showed type 2 fluorescence changes upon stimulation; these are better illustrated by changes in the total fluorescence of the vesicle (Fig. 6B). Therefore, in this set of experiments, the total fluorescence of vesicles was analyzed by Metamorph (see Materials and Methods).

In the cells that overexpressed wild-type Rab3A, the extent of decrease in the total fluorescence in the evanescence field was similar to that of the control cells, but the initial rate of decrease was slower (Fig. 6A). For the single vesicles with type 2 fluorescence change, there was an average increase of more than 50% in the fluorescence of NPY-EGFP-labeled vesicles, which occurred within 1 sec and then there was a decrease to the background level in $<$3 sec (Fig. 6B,C).

For cells that overexpressed Rab3A Q81L, the total fluorescence in the evanescent field did not change significantly suggesting that the exocytotic activity was decreased (Fig. 6A, Video 5), but there were a few vesicles that did undergo exocytosis, which showed a similar pattern to NPY-EGFP fluorescence change as that in the controls (cells transfected with wild type Rab3A) (Fig. 6B,C). It should be noted that we did not find any Rab3A Q81L-labeled vesicles with fluorescence dispersion (Fig. 5D). It is possible that the vesicles that underwent exocytosis did this mediated by endogenous wild-type Rab3A. Alternatively, GTPase-activating protein may activate the Rab3A Q81L GTPase activity, although to a lower extent than the wild-type (Brondyk et al., 1993). This would cause GTP hydrolysis and then dissociation of the protein from the vesicles. Additionally, GDI may induce the dissociation of a small number of Rab3A Q81L protein molecules from the vesicles (Araki et al., 1990) and allow these vesicles to proceed to exocytosis.

In Rab3A T36N overexpressing cells, the total fluorescence in the evanescent field showed a smaller transient increase but the extent of fluorescence decrease was similar to that of the control cells (Fig. 6A), which is in accord with the results from previous studies. In these studies, overexpression of Rab3A T36N did not inhibit stimulated secretion in chromaffin cells and PC12 cells (Holz et al., 1994; Johannes et al., 1994; Schlüter et al., 2002). Furthermore, two thirds of the NPY-EGFP vesicles that were identified as undergoing exocytosis showed a fluorescence decrease without the transient increase, which was higher than that observed in the cells that overexpressed wild type Rab3A and the other mutants, ~50% (Video 7). The single vesicle analysis showed that the fluorescence of type 2 vesicles appeared to decrease faster than the vesicles in wild type Rab3A-expressing cells (Fig. 6B,C). This may be accounted for by the release of NPY-EGFP becoming faster.

It is interesting that for the Rab3A F59S-overexpressed cells, the type 2 NPY-EGFP fluorescence transients stayed bright for a longer, and the fluorescence then returned to a much higher level than cells transfected with wild type Rab3A and the other mutants (Fig. 6B,C). The results suggest that the interaction of Rab3A with rabphilin is not only involved in the process of Rab3A dissociation (Fig. 5D) but also in the process of NPY release.

Discussion

Using TIRFM, we were able to visualize the dissociation of Rab3A from vesicles and NPY release in living cells. We have

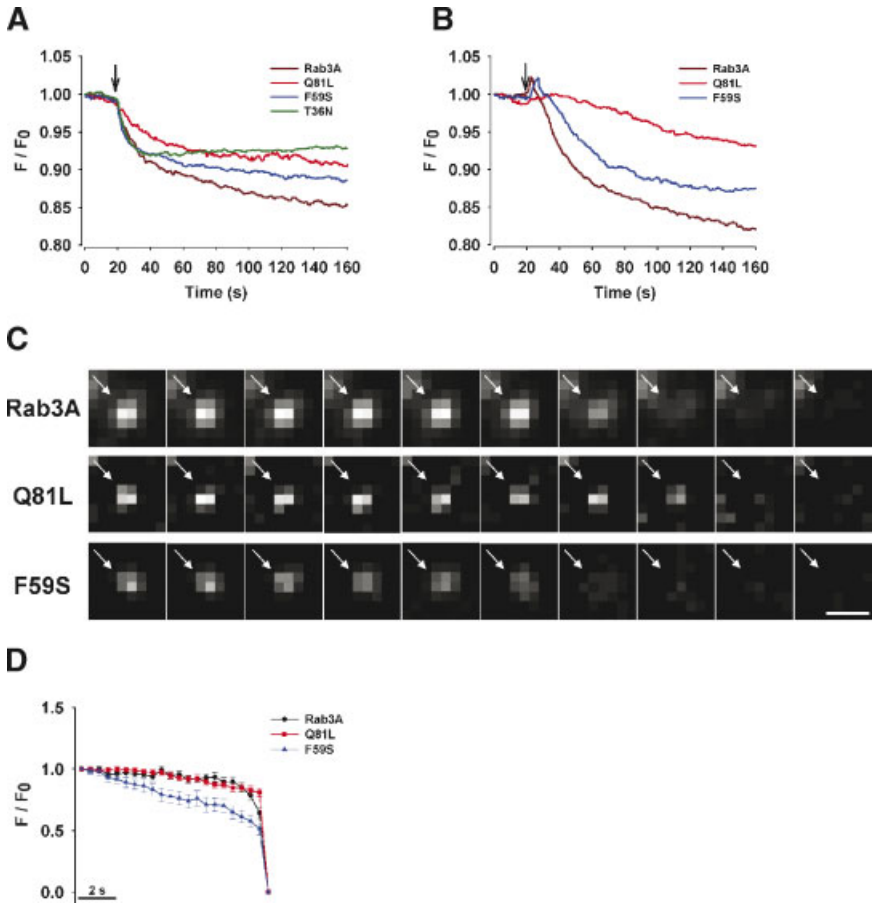

Fig. 5. Changes in the fluorescence of EGFP-Rab3A or mutants upon ATP stimulation. PC12 cells transfected with pEGFP-Rab3A or its mutants were stimulated by ATP. Images were acquired by TIRFM and the total fluorescence in the evanescent field was analyzed by MetaMorph. There were two major patterns of changes: A: Fluorescence decreased gradually. The data shown are the mean ± SEM from 19, 7, 20, and 22 cells overexpressing wild-type Rab3A, Rab3AQ81L, Rab3A F59S, and Rab3A T36N, respectively. B: Fluorescence increased transiently before the decrease. The data shown are the mean ± SEM from 16, 21, and 24 cells overexpressing wild-type Rab3A, Rab3AQ81L, and Rab3A F59S, respectively. Fluorescence (F) was normalized to the level at resting level (F_0). C: Representative images of single vesicle from cells transfected with Rab3A or mutants. D: Averaged fluorescence changes of single vesicles. Fluorescence of single vesicles in the TIRFM images were tracked and analyzed by DiaTrack. The fluorescence intensity of vesicles that disappeared after stimulation from cells that overexpressing the wild-type or mutant Rab3A were synchronized at the frame before the abrupt decrease in fluorescence. Fluorescence (F) was normalized to the level at resting level (F_0). The data shown are the mean ± SEM from 37, 32, and 30 vesicles for wild-type, Rab3A Q81L, and Rab3A F59S, respectively.

carried out a detailed analysis of the changes in total fluorescence across the evanescent field and the fluorescence of single vesicles. The fluorescence changes of single vesicles can be divided into different types. For the three types of the NPY-EGFP fluorescence changes, it is possible that the size of the fusion pore and/or the opening time of the fusion pore are different and this causes the release of NPY at different rates and to different extents. Type 1 has been shown in PC12 cells and bovine chromaffin cells; previous results suggest that it is due to the recapture of the vesicle after exocytosis (Holroyd et al., 2002; Taraska et al., 2003; Perrais et al., 2004). The type 2 fluorescence transient has been shown for NPY-EGFP-labeled vesicles in PC12 cells (Taraska et al., 2003), FM1-43 stained synaptic vesicles in retinal bipolar cells (Zenisek et al., 2002), and acridine orange/phogrin-EGFP labeled insulin vesicles (Tsuboi et al., 2004). The type 2 transients appear to be due to the alkalization of the acidic pH in the vesicle during exocytosis as has been suggested elsewhere (Barg et al., 2002; Taraska et al., 2003). However, a contribution by the movement of vesicles toward plasma membrane cannot be excluded. Our results showed that stimulation induced a higher level of fluorescence increase than that induced by NH_4Cl and the transient increase was similar at both pH 5.5 and 7.4.

For the changes of EGFP-Rab3A fluorescence at the single vesicle level, the dispersion and decrease of EGFP-Rab3A fluorescence is taken to represent the dissociation of Rab3A from the vesicles. However, it is not clear when Rab3A leaves the vesicles during the secretory process and whether Rab3A diffuses into the plasma membrane before its dissociation into the cytosol. Our preliminary results (Huang and co-workers) obtained by simultaneously monitoring Rab3A and NPY at the single vesicle level have shown that Rab3A remained in the vesicles when NPY-EGFP transients appeared, which represents the time when fusion occurs. Therefore, it is likely that Rab3A did not leave the vesicle before fusion.

Two major types of changes in the total fluorescence were observed when NPY-EGFP and EGFP-Rab3A-expressed cells were stimulated. The biological significance of the two types of NPY-EGFP fluorescence changes is not clear. For the changes in the total fluorescence of EGFP-Rab3A, the transient increase may result from the movement of vesicles toward the plasma membrane upon stimulation. No Rab3A T36N-overexpressed

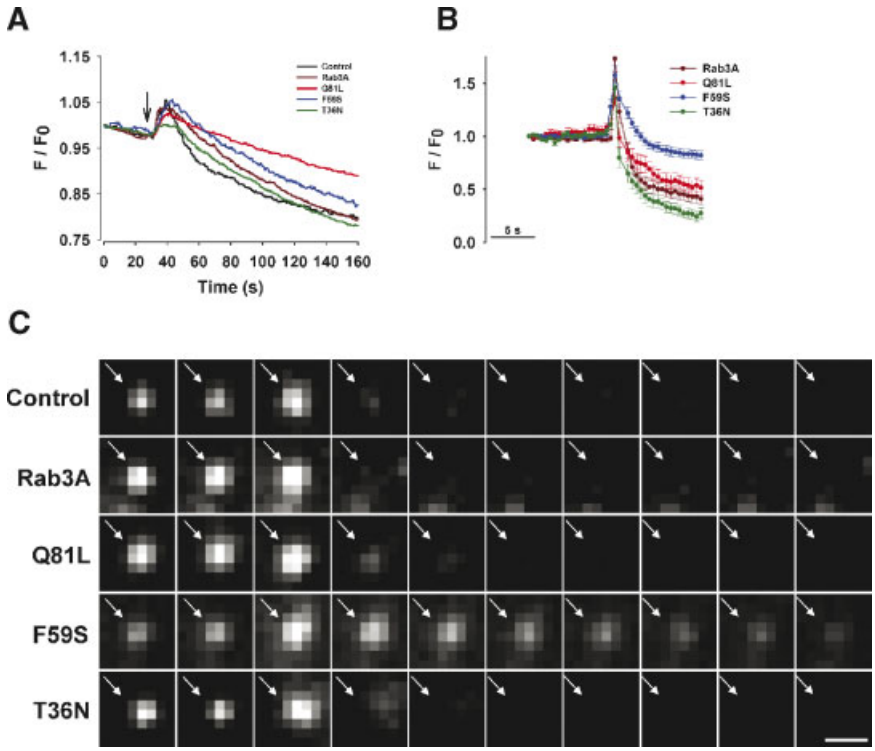

Fig. 6. Effects of overexpression of Rab3A or mutants on NPY-EGFP-labeled vesicles upon stimulation. PC12 cells co-transfected with pNPY-EGFP and pECFP-Rab3A or mutants, were stimulated with ATP as described in Figure 5. The fluorescence changes of NPY-EGFP were detected by TIRFM at ~2 frame/s. A: Total fluorescence in the evanescent field. Results from all cells that showed fluorescence change >3% of the initial level were averaged. B: Averaged fluorescence changes of single vesicles. Individual NPY-EGFP-labeled vesicles that showed type 2 transient fluoresence change upon stimulation were identified and analyzed by MetaMorph. Fluorescence (F) was normalized to the level at resting level (F_0). The data shown are the mean ± SEM from 22, 29, and 28 vesicles for wild type Rab3A, Rab3A F59S, and Rab3A T36N-overexpressed cells, respectively. For Rab3A Q81L-overexpressed cells, only 16 vesicles were analyzed because the number of vesicles that proceed to exocytosis was significantly decreased. The fluoresence changes were aligned at the frame that showed highest fluorescence level. C: Representative images of single NPY-EGFP-labeled vesicle from cells that overexpressed wild type Rab3A or mutants as indicated.

cells were found to show the transient increase in their total fluorescence and this is compatible with a transient increase due to the movement of vesicles toward the plasma membrane because Rab3A T36N is located in the plasma membrane and cytosol (Fig. 4C,G).

The results from the two mutants related to the nucleotide binding state of Rab3A, GTP-bound Rab3A Q81L and GDP-bound Rab3A T36N, provide direct evidence for our current understanding of the molecular mechanism of Rab3A. We showed that Rab3A Q81L was bound to the vesicles and did not dissociate from the vesicle upon stimulation. Exocytosis was inhibited in cells that overexpressed Rab3A Q81L. These results are direct in vivo evidence confirming that the dissociation of Rab3A requires GTP hydrolysis and that the vesicles with GTP-Rab3A bound are not able to proceed to exocytosis.

Rab3A T36N was shown to be present in the cytosol and plasma membrane (Fig. 4C,G) and the fluorescence of EGFP-Rab3A T36N in the evanescent field decreased upon stimulation (Fig. 5A). In cells overexpressing the GDP-bound mutant, two thirds of the vesicles that exocytosed showed no transient increase in NPY-EGFP fluorescence during exocytosis, which suggests that fusion and release are faster than in the control cells so that the probability of the transient to be captured by camera becomes less. These results suggest that after GTP hydrolysis, GDP-bound Rab3A remained in the plasma membrane, and help the formation of fusion complexes. Rab3A has been shown to be involved in either the formation of the SNARE complex or it may control the stability of the SNARE complex (Johannes et al., 1996).

Results from the two mutants demonstrate that GTP hydrolysis is crucial for Rab3A acting as a gatekeeper for the occurrence of exocytosis. Our results provide in vivo evidence to confirm the conclusions obtained from previous in vitro biochemical results, namely, that free Rab3A in the cytosol is the GDP-bound form and the Rab3A that binds to synaptic vesicles is mainly the GTP-bound form (Fischer von Mollard et al., 1991; Stahl et al., 1994; Chou and Jahn, 2000). In addition, GDP-bound Rab3A binds to membrane and Rab3 GDI retrieves the GDP-bound Rab3A from membrane more easily in presence of Ca^{2+} (Park et al., 1997; Sakisaka et al., 2002). The results are also is in accord with previous results that firstly, without Rab3A dissociation, α-latrotoxin still induces fusion in the absence of Ca^{2+} and secondly, the Rab3A bound to the plasma membrane, possibly on the docked vesicles, shifts from the GTP-bound to the GDP-bound form (Stahl et al., 1994). Rabphilin was identified by its interaction with Rab3A, however, its role in secretion and the function of its interaction with Rab3A is not completely understood. Our results show that in the absence of interaction with rabphilin, Rab3A dissociation has two phases (Fig. 5D), which may affect vesicle docking and thus causes an inhibition of secretion. Furthermore, the NPY-EGFP fluorescence transient events became larger and broader (Fig. 6B,C), which showed that fusion is able to occur but the rate of release is inhibited by the mutant. It has been shown that rabphilin promotes secretion via the C2A domain,

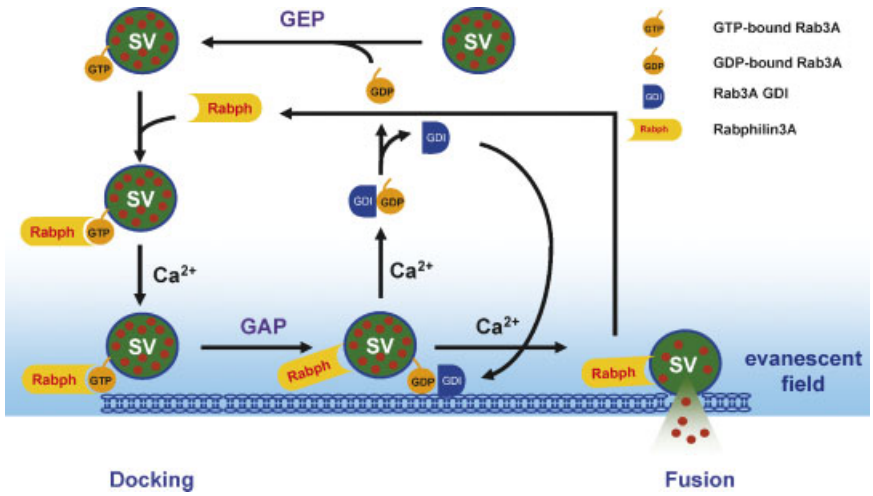

Fig. 7. Working hypothesis of the role of Rab3A in regulated secretion. GTP-bound Rab3A binds to vesicles, which recruits rabphilin3A before docking on the plasma membrane. When cytosolic Ca^{2+} is increased by stimulation, rabphilin and GTPase-activating protein (GAP) increase the rate of GTP hydrolysis and renders Rab3A GDP-bound. Guanine nucleotide dissociation inhibitor (GDI) is then activated, possibly by cytosolic Ca^{2+}, to retrieve Rab3A from vesicle membrane. In the mean time, vesicles are able proceed to fusion and there is exocytosis of NPY via Rab3A-activated rabphilin under a high concentration of cytosolic Ca^{2+}.

the Ca^{2+} sensor in synaptotagmin, by overexpression of rabphilin and its mutants in chromaffin cells (Chung et al., 1995). Using a rabphilin homolog-disrupted *C. elegans* mutant, Staunton et al. (2001) provided evidence to show that rabphilin interacts with the components of the SNARE complex, which is independent of Rab3A. It is possible that rabphilin3A promotes dilation of the fusion pore via C2A by mechanisms similar to that of synaptotagmin (Wang et al., 2003). Our results together with previous results support the view that rabphilin acts as a positive regulator of secretion in both a Rab3A-dependent and a Rab3A-independent way. Rabphilin requires GTP-bound Rab3A to interact with the vesicles and after GTP hydrolysis, rabphilin dissociates from Rab3A but remain on the vesicle to regulate fusion pore formation.

In summary, we have provided direct evidence to demonstrate that GTP hydrolysis is critical for the dissociation of Rab3A from the vesicles, GDP-bound Rab3A remained on the plasma membrane and rabphilin is involved in the dissociation of Rab3A and the exocytosis. Based on these results, we have refined the current working hypothesis on the action of Rab3A in the secretory process (Fig. 7). GTP-bound Rab3A binds to secretory vesicles and recruits rabphilin to help vesicles to dock on the membrane. GTP hydrolysis occurs somewhere along the way to convert the GTP-bound to GDP-bound Rab3A. After GTP hydrolysis, several events occur and vesicles are able to proceed to exocytosis. Rabphilin dissociates from Rab3A but remains on the vesicle. GDP-Rab3A moves to the plasma membrane and helps the formation of the fusion pore. When cytosolic Ca^{2+} is increased upon stimulation, GDI is activated to remove GDP-bound Rab3A from membrane and rabphilin and other components of SNARE complex are activated by synaptotagmin and participate in subsequent fusion pore dilation and NPY release. In this study, the Rab3A dissociation was visualized and this provides an excellent system for further studies of the secretory process.

Acknowledgments

We thank Dr. W. Almers and Dr. Südhof for providing pEGFP-N1-NPY and Rab3A mutants; and Dr. W.J. Betz, Dr. W. Almers, Dr. M.J. Fann and Dr. C.-Y. Pan for the suggestions about the experiments and valuable comments.

Literature Cited

Allersma MW, Wang L, Axelrod D, Holz RW. 2004. Visualization of regulated exocytosis with a granule-membrane probe using total internal reflection microscopy. Mol Biol Cell 15:4658–4668.

Araki S, Kikuchi A, Hata Y, Isomura M, Takai Y. 1990. Regulation of reversible binding of smg p25A, a ras p21-like GTP-binding protein, to synaptic plasma membranes and vesicles by its specific regulatory protein, GDP dissociation inhibitor. J Biol Chem 265:13007–13015.

Barg S, Olofsson CS, Schriever-Abeln J, Wendt A, Gebre-Medhin S, Renstrom E, Rorsman P. 2002. Delay between fusion pore opening and peptide release from large dense-core vesicles in neuroendocrine cells. Neuron 33:287–299.

Brondyk WH, McKiernan CJ, Burstein ES, Macara IG. 1993. Mutants of Rab3A analogous to oncogenic Ras mutants. Sensitivity to Rab3A-GTPase activating protein and Rab3A-guanine nucleotide releasing factor. J Biol Chem 268:9410–9415.

Chou JH, Jahn R. 2000. Binding of Rab3A to synaptic vesicles. J Biol Chem 275:9433–9440.

Chung SH, Takai Y, Holz RW. 1995. Evidence that the Rab3a-binding protein, rabphilin3a, enhances regulated secretion. Studies in adrenal chromaffin cells. J Biol Chem 270:16714–16718.

Chung SH, Joberty G, Gelino EA, Macara IG, Holz RW. 1999. Comparison of the effects on secretion in chromaffin and PC12 cells of Rab3 family members and mutants. Evidence that inhibitory effects are independent of direct interaction with Rabphilin3. J Biol Chem 274:18113–18120.

Coppola T, Hirling H, Perret-Menoud V, Gattesco S, Catsicas S, Joberty G, Macara IG, Regazzi R. 2001. Rabphilin dissociated from Rab3 promotes endocytosis through interaction with Rabaptin-5. J Cell Sci 114:1757–1764.

Coppola T, Frantz C, Perret-Menoud V, Gattesco S, Hirling H, Regazzi R. 2002. Pancreatic beta-cell protein granuphilin binds Rab3 and Munc-18 and controls exocytosis. Mol Biol Cell 13:1906–1915.

Fischer von Mollard G, Sudhof TC, Jahn R. 1991. A small GTP-binding protein dissociates from synaptic vesicles during exocytosis. Nature 349:79–81.

Geppert M, Südhof TC. 1998. RAB3 and synaptotagmin: The yin and yang of synaptic membrane fusion. Annu Rev Neurosci 21:75–95.

Geppert M, Bolshakov VY, Siegelbaum SA, Takei K, De Camilli P, Hammer RE, Südhof TC. 1994. The role of Rab3A in neurotransmitter release. Nature 369:493–497.

Geppert M, Goda Y, Stevens CF, Südhof TC. 1997. The small GTP-binding protein Rab3A regulates a late step in synaptic vesicle fusion. Nature 387:810–814.

Holroyd P, Lang T, Wenzel D, De Camilli P, Jahn R. 2002. Imaging direct, dynamin-dependent recapture of fusing secretory granules on plasma membrane lawns from PC12 cells. Proc Natl Acad Sci USA 99:16806–16811.

Holz RW, Brondyk WH, Senter RA, Kuizon L, Macara IG. 1994. Evidence for the involvement of Rab3A in Ca^{2+}-dependent exocytosis from adrenal chromaffin cells. J Biol Chem 269:10229–10234.

Johannes L, Lledo PM, Roa M, Vincent JD, Henry JP, Darchen F. 1994. The GTPase Rab3a negatively controls calcium-dependent exocytosis in neuroendocrine cells. EMBO J 13:2029–2037.

Johannes L, Doussau F, Clabecq A, Henry JP, Darchen F, Poulain B. 1996. Evidence for a functional link between Rab3 and the SNARE complex. J Cell Sci 109:2875–2884.

Johnston PA, Archer BTIII,Robinson K, Mignery GA, Jahn R, Südhof TC. 1991. Rab3A attachment to the synaptic vesicle membrane mediated by a conserved polyisoprenylated carboxy-terminal sequence. Neuron 7:101–109.

Lang T, Wacker I, Steyer J, Kaether C, Wunderlich I, Soldati T, Gerdes HH, Almers W. 1997. Ca^{2+}-triggered peptide secretion in single cells imaged with green fluorescent protein and evanescent-wave microscopy. Neuron 18:857–863.

Leenders AG, Lopes da Silva FH, Ghijsen WE, Verhage M. 2001. Rab3a is involved in transport of synaptic vesicles to the active zone in mouse brain nerve terminals. Mol Biol Cell 12:3095–3102.
Lin CG, Pan CY, Kao LS. 1996. Rab3A delayed catecholamine secretion from bovine adrenal chromaffin cells. Biochem Biophys Res Commun 221:675–681.
Macara IG. 1994. Role of the Rab3A GTPase in regulated secretion from neuroendocrine cells. Trends Endocrinol Metab 5:267–271.
Matteoli M, Takei K, Cameron R, Hurlbut P, Johnston PA, Südhof TC, Jahn R, De Camilli P. 1991. Association of Rab3A with synaptic vesicles at late stages of the secretory pathway. J Cell Biol 115:625–633.
Ohara-Imaizumi M, Nishiwaki C, Kikuta T, Kumakura K, Nakamichi Y, Nagamatsu S. 2004. Site of docking and fusion of insulin secretory granules in live MIN6 beta cells analyzed by TAT-conjugated anti-syntaxin 1 antibody and total internal reflection fluorescence microscopy. J Biol Chem 279:8403–8408.
Ohya T, Sasaki T, Kato M, Takai Y. 1998. Involvement of Rabphilin3 in endocytosis through interaction with Rabaptin5. J Biol Chem 273:613–617.
Park JB, Farnsworth CC, Glomset JA. 1997. Ca^{2+}/calmodulin causes Rab3A to dissociate from synaptic membranes. J Biol Chem 272:20857–20865.
Patterson GH, Knobel SM, Sharif WD, Kain SR, Piston DW. 1997. Use of the green fluorescent protein and its mutants in quantitative fluorescence microscopy. Biophys J 73:2782–2790.
Perrais D, Kleppe IC, Taraska JW, Almers W. 2004. Recapture after exocytosis causes differential retention of protein in granules of bovine chromaffin cells. J Physiol 560:413–428.
Südhof TC. 2004. The synaptic vesicle cycle. Annu Rev Neurosci 27:509–547.
Sakisaka T, Meerlo T, Matteson J, Plutner H, Balch WE. 2002. Rab-alphaGDI activity is regulated by a Hsp90 chaperone complex. EMBO J 21:6125–6135.
Sankaranarayanan S, De Angelis D, Rothman JE, Ryan TA. 2000. The use of pHluorins for optical measurements of presynaptic activity. Biophys J 79:2199–2208.
Schlüter OM, Khvotchev M, Jahn R, Südhof TC. 2002. Localization versus function of Rab3 proteins. Evidence for a common regulatory role in controlling fusion. J Biol Chem 277:40919–40929.
Slembrouck D, Annaert WG, Wang JM, Potter WP. 1999. Rab3 is present on endosomes from bovine chromaffin cells in primary culture. J Cell Sci 112:641–649.
Stahl B, von Mollard GF, Walch-Solimena C, Jahn R. 1994. GTP cleavage by the small GTP-binding protein Rab3A is associated with exocytosis of synaptic vesicles induced by alpha-latrotoxin. J Biol Chem 269:24770–24776.
Staunton J, Ganetzky B, Nonet ML. 2001. Rabphilin potentiates soluble N-ethylmaleimide sensitive factor attachment protein receptor function independently of rab3. J Neurosci 21:9255–9264.
Steyer JA, Horstmann H, Almers W. 1997. Transport, docking and exocytosis of single secretory granules in live chromaffin cells. Nature 388:474–478.
Taraska JW, Perrais D, Ohara-Imaizumi M, Nagamatsu S, Almers W. 2003. Secretory granules are recaptured largely intact after stimulated exocytosis in cultured endocrine cells. Proc Natl Acad Sci USA 100:2070–2075.
Tsuboi T, McMahon HT, Rutter GA. 2004. Mechanisms of dense core vesicle recapture following "kiss and run" ("cavicapture") exocytosis in insulin-secreting cells. J Biol Chem 279:47115–47124.
Wang CT, Lu JC, Bai J, Chang PY, Martin TF, Chapman ER, Jackson MB. 2003. Different domains of synaptotagmin control the choice between kiss-and-run and full fusion. Nature 424:943–947.
Yang DM, Huang CC, Lin HY, Tsai DP, Kao LS, Chi CW, Lin CC. 2003. Tracking of secretory vesicles of PC12 cells by total internal reflection fluorescence microscopy. J Microsc 209:223–227.
Zenisek D, Steyer JA, Feldman ME, Almers WA. 2002. Membrane marker leaves synaptic vesicles in milliseconds after exocytosis in retinal bipolar cells. Neuron 35:1085–1097.